University of Kent

Kent Academic Repository

Wang, Guoqing, Shao, Liyang, Liu, Yibing, Xu, Weijie, Xiao, Dongrui, Liu, Shuaiqi, Hu, Jie, Zhao, Fang, Shum, Ping, Wang, Weizhi and others (2021) *Low-cost compressive sensing imaging based on spectrum-encoded time-stretch structure.* Optics Express, 29 (10). p. 14931. ISSN 1094-4087.

Downloaded from

https://kar.kent.ac.uk/92167/ The University of Kent's Academic Repository KAR

The version of record is available from

https://doi.org/doi:10.1364/OE.421055

This document version

Publisher pdf

DOI for this version

Licence for this version

CC BY (Attribution)

Additional information

Versions of research works

Versions of Record

If this version is the version of record, it is the same as the published version available on the publisher's web site. Cite as the published version.

Author Accepted Manuscripts

If this document is identified as the Author Accepted Manuscript it is the version after peer review but before type setting, copy editing or publisher branding. Cite as Surname, Initial. (Year) 'Title of article'. To be published in ***Title of Journal*** , Volume and issue numbers [peer-reviewed accepted version]. Available at: DOI or URL (Accessed: date).

Enquiries

If you have questions about this document contact ResearchSupport@kent.ac.uk. Please include the URL of the record in KAR. If you believe that your, or a third party's rights have been compromised through this document please see our Take Down policy (available from https://www.kent.ac.uk/guides/kar-the-kent-academic-repository#policies).

Research Article | Vol. 29, No. 10 / 10 May 2021 / Optics Express 14931
Optics EXPRESS

Low-cost compressive sensing imaging based on spectrum-encoded time-stretch structure

GUOQING WANG,[1] LIYANG SHAO,[1,2,*] YIBING LIU,[1] WEIJIE XU,[1] DONGRUI XIAO,[1] SHUAIQI LIU,[1] JIE HU,[1] FANG ZHAO,[1] PING SHUM,[1] WEIZHI WANG,[2] YUAN ZHOU,[3] RUI MIN,[4] AND CHAO WANG[5]

[1]*School of Electronic and Electrical Engineering, Southern University of Science and Technology, Shenzhen, 518055, China*
[2]*Peng Cheng Laboratory, Shenzhen 518055, Guangdong, China*
[3]*Department of Periodontology, Shenzhen Stomatological Hospital, Southern Medical University, Shenzhen, 518005, China*
[4]*Center for Cognition and Neuroergonomics, State Key Laboratory of Cognitive Neuroscience and Learning, Beijing Normal University at Zhuhai, Zhuhai, 519087, China*
[5]*School of Engineering and Digital Arts, University of Kent, Canterbury, CT2 7NT, United Kingdom*
[*]*shaoly@sustech.edu.cn*

Abstract: A low-cost compressive sensing imaging (CSI) system based on spectrum-encoded time-stretch (SETS) structure involving cascaded Mach-Zehnder Interferometers (MZIs) for spectral domain random mixing (also known as the optical random pattern generator) is proposed and experimentally demonstrated. A proof-of-principle simulation and experiment is performed. A mode-locked laser with a repetition rate of 50MHz and low-cost cascaded MZIs as the key devices enable fast CSI system. Data compression ratio from 6% to 25% are obtained using proposed CSI based SETS system. The proposed design solves the big data issue in the traditional time-stretch system. It has great potential in fast dynamic phenomena with low-cost and easy-access components.

Published by The Optical Society under the terms of the Creative Commons Attribution 4.0 License. Further distribution of this work must maintain attribution to the author(s) and the published article's title, journal citation, and DOI.

1. Introduction

Serial time-encoded amplified microscopy (STEAM) based on the spectrum-encoded time-stretch (SETS) structure, which enabled extraordinary ultrafast imaging speed of hundreds of tens of MHz or even GHz [1] and has been employed in widely useful applications, especially in ultrafast optical imaging and dynamic phenomena detection, such as ultrafast laser scanning [2], flowing particle screening [3], ultrafast optical imaging [4–12], ultrafast quantitative cellular and tissue imaging [13] based on phase-sensitive manipulation [14,15], light ranging [16] and compressive sensing imaging [17–19]. STEAM can be divided into two steps: one-to-one mapping between spectrum and space, also known as spectrum encoded procession, or space to spectrum conversion; one-to-one mapping between spectrum and time mapping, also known as time-stretch procession, or spectrum to time conversion. The spectrum encoded procession encodes the spatial imaging information into broadband optical spectrum using diffractive optical devices, such as free-space diffractive grating [20] and in-fiber diffraction grating [21–24] for 1D imaging, and virtually imaged phased array (VIPA) and a diffractive grating for 2D imaging [1]; and the time-stretch procession encodes the space-modulated broadband optical spectrum information into time serial using optical devices, such as dispersive compensating fiber (DCF) [4–12]. As a result, the one-to-one mapping among space to time is achieved via the usage

#421055 https://doi.org/10.1364/OE.421055
Journal © 2021 Received 25 Feb 2021; revised 5 Apr 2021; accepted 17 Apr 2021; published 29 Apr 2021

Optics EXPRESS

of spectrum of the optical light. Hence, an ultrafast single-pixel detector, for example, an photodetector (PD) can be utilized to detect the ultrafast optical dynamic phenomena.

However, conventionally the implementation of time-stretch procession demands ultrafast PDs and oscilloscopes, which normally are expensive. This drastically increases the cost of the optical system. Also great amount of data that gathered by conventional optical imaging systems needs to be processed by high speed data acquisition cards. The commonly applied solution is based on nonlinear one-to-one mapping between time and spectrum, such as anamorphic stretched transform or wrapped time stretch [25,26]. Also, much more useful information could be detected as well as with better temporal resolution. The other solution involving designed algorithms, such as the utilization of the compressive sensing (CS) method [17,27–29], which drastically reduces the great amount of data that needs to be acquired, has the benefits of low-cost due to the employment of low-cost low-bandwidth PDs and oscilloscopes. For example, a low-cost low-bandwidth of 50 MHz PD can be employed as the substitute of the traditional expensive high-bandwidth PD when using CS method. In order to perform compressive sensing imaging (CSI), pseudorandom binary sequences (PRBS) that used to generate optical random patterns are essential for the CS procession [27–30]. Previously, the arbitrary waveform generators (AWGs) generate PRBS sequences could achieve a high speed of 10 GHz or even more. Also, costly high-speed electro-optical modulators are required to perform high speed modulation. As a result, previous approach for ultrafast speed imaging and dynamic phenomena detection has the drawback of expensive.

To tackle this issue, an optical random pattern generator based on cascaded Mach-Zehnder interferometers (MZIs) [30–32], which eliminates the usage of AWGs and expensive large-bandwidth modulators, with the benefit of easy-access and low-cost is proposed. Note here the two low-cost customer designed MZIs are consists of two 1×2 optical fiber couplers and one 2×2 optical fiber coupler, instead of two expensive Mach-Zehnder Modulators (MZMs), which are quite expensive.

In this Letter, based on our previous work [4,5,17], we propose and experimentally demonstrate an optical CSI system based on SETS structure. An optical random pattern generator based on cascaded MZIs structure is employed to perform the low-cost optical mixing. The experimental CSI results indicating a data compression ratio from 6% to 25% is obtained with an imaging area of 0.6*2.2 mm. This method has wide applications in dynamic phenomena where low-cost, easy-access and high-speed system is required.

2. Experimental section

The schematic of the proposed PRBS generation system using cascaded MZIs structure is shown in Fig. 1. A pulsed mode-locked laser (MLL, Er-Femto EFLA laser) with a repetition rate of 50 MHz is employed as the laser source, which has a maximum optical power of 200 mW and the pulses produced by MLL have a full-width at half maximum (FWHM) of 44 fs. In order to achieve linear one-to-one mapping between spectrum and time, ultrashort optical pulses from MLL are stretched in time domain using dispersive compensating fibers (DCFs, with a total dispersion of 0.32 ns/nm). The dispersion also lays solid foundation for signal loading and data detection. Besides, one Erbium doped fiber amplifier (EDFA) is used for optical amplification to achieve higher signal-to-noise ratio (SNR).

The amplified and time-stretched optical pulses pass the cascaded MZIs, where the pulses are modulated by the signals, and then the random optical patterns are generated. The signals can be loaded via PZT with different modulation frequency and intensity, or changing the optical path difference (OPD) using variable delay line (VDL) device. In our proposal, the method of changing OPD using VDL device from 1 mm to 50 mm with a step of 1 mm is applied. Compared to MZ modulators, the fiber-based cascaded MZIs needs isolation of temperature variation, vibration and sound to prevent the influence of the environment. The isolation process, also

Optics EXPRESS

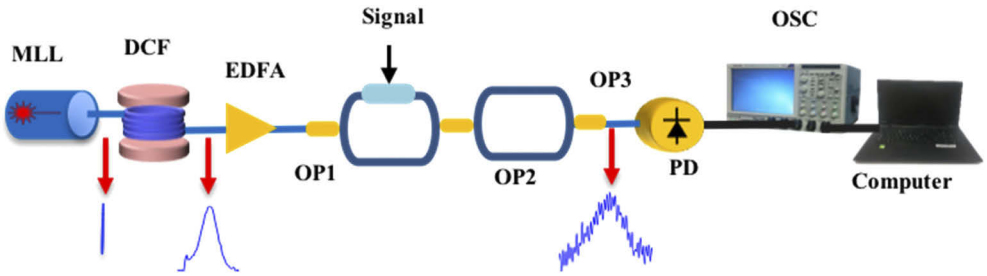


Fig. 1. Schematic of the proposed random optical pattern generation process

known as capsulation process, is achieved by putting the whole MZIs structure into one box with full of foam or sponge, which could isolate the environmental temperature variation, vibration and sound. And in the past this capsulation method could load the signals into Michelson interferometer for sensing applications [33]. After the cascaded MZIs, the PRBS waveform is detected by the PD and followed by Oscilloscope and saved by computer.

The output of time-stretched pulses in spectral domain before and after pass through the cascaded MZIs (where PRBS modulation process obtained) are shown in Fig. 2(a) and 2(b), respectively. Figure 2(a) shows the spectrum of the MLL before the PRBS modulation, and the 3dB spectrum is 15nm. Figure 2(b) shows the spectrum of the MLL after the PRBS modulation, and 23 free spectral ranges (FSRs) are observed clearly over the full spectrum after PRBS modulation. The output temporal waveform of the time-stretched pulses without and with PRBS modulation is shown in Fig. 2(c) and 2(d), respectively. Figure 2(c) depicts the laser pulse is a gaussian pulse without PRBS modulation and each optical pulse has a period of 20ns and the 3dB pulse lasts around 6ns. Figure 2(d) illustrates the temporal waveform of time-stretched pulses after passed the cascaded MZIs structure and after PRBS modulation 33 FSRs can be observed in a period of 20ns. The red square parts in Fig. 2(c) and 2(d) are expanded for compare the details of influence of with and without PRBS modulation on the time-stretched temporal pulses.

To verify the quality of the random patterns (shown in Fig. 2(d)) that generated by the cascaded MZIs, 100 modulated and continuous optical pulses that pass through the cascaded MZIs with varied OPDs (from 0.5 mm to 50 mm with a step of 0.5 mm) are detected and their correlation coefficient are measured in Matlab. Figure 3 shows the result of pattern correlation coefficient of 100 continuous optical pulses. The results describe a mean value of 0.28, which obviously confirm the random patterns that generated by cascaded MZIs are perfect candidates for low-cost CSI. Note whether in spectral domain or time domain, there are interference fringes resulting from the interference of the cascaded MZIs. As a result, the random patterns are generated. For ultrafast imaging detection, data acquisition in time domain is enough due to the one-to-one linear mapping among spectrum, space and time. Also, due to the one-to-one mapping between spectrum and time, only one domain analysis is required. In spectral domain, the free spectral range (FSR) in terms of optical spectrum is shown as $\Delta\lambda=\lambda\hat{}2/2\ \Delta l$, where Δl is the OPD of two interferometric arms; λ is the optical wavelength. In our experiment, the λ has a range of 15nm (from 1556nm to 1571nm). As a result, perfect random patterns for CSI are generated when the signals are loaded into the pulses via the cascaded MZIs. The signals are loaded via PZT with different modulation frequency and intensity, and manually added the modulation frequency and intensity again for confirmation, and another confirmation is done with varied OPDs.

The schematic of the proposed CSI system based on SETS structure is shown in Fig. 4. In the experiment, the PRBS waveforms are already reserved in a database and with same OPDs the waveforms show great consistence when time changes [30,31]. The PRBS generation system is same as Fig. 1. Note here synchronization process is required, one RF signal channel directly

Optics EXPRESS

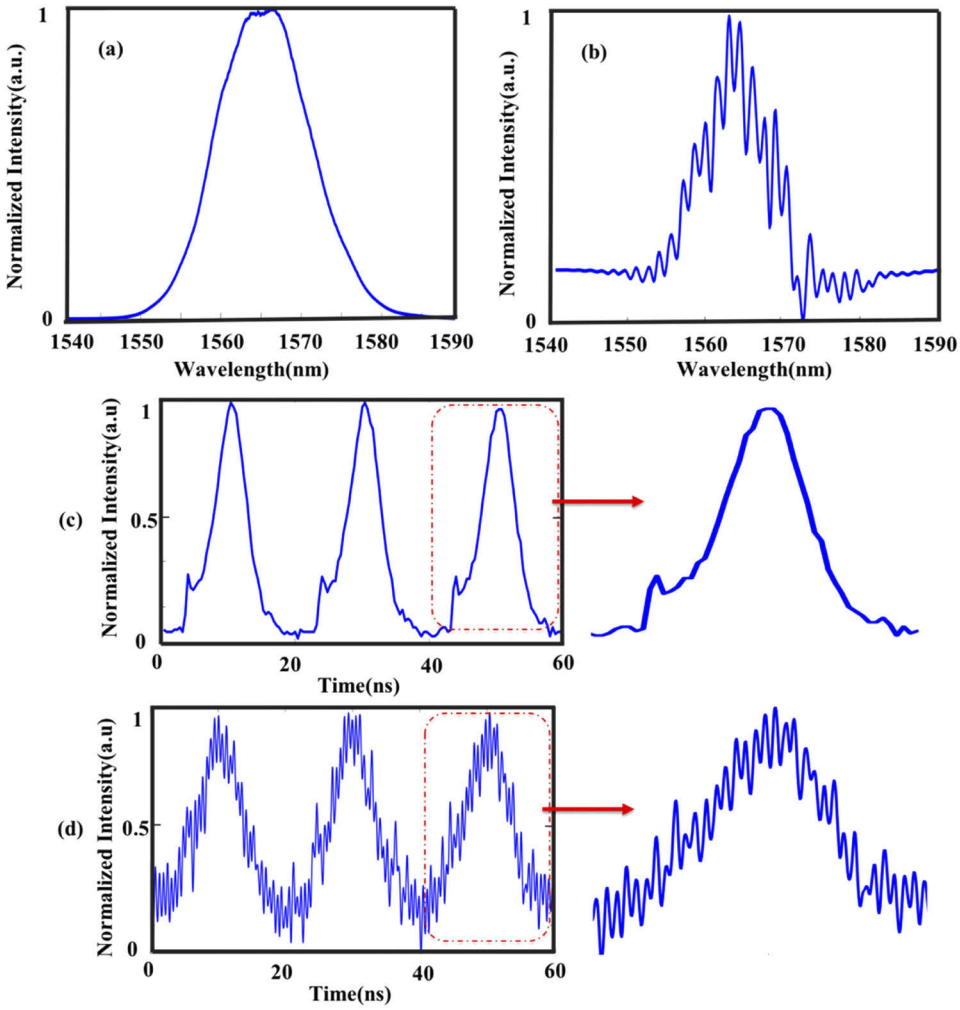


Fig. 2. Output spectrum of the MLL source before (a) and after (b) PRBS modulation; output temporal waveform of the MLL source after time-stretch (c) without and (d) with PRBS modulation. MLL: mode-locked laser.

Optics EXPRESS

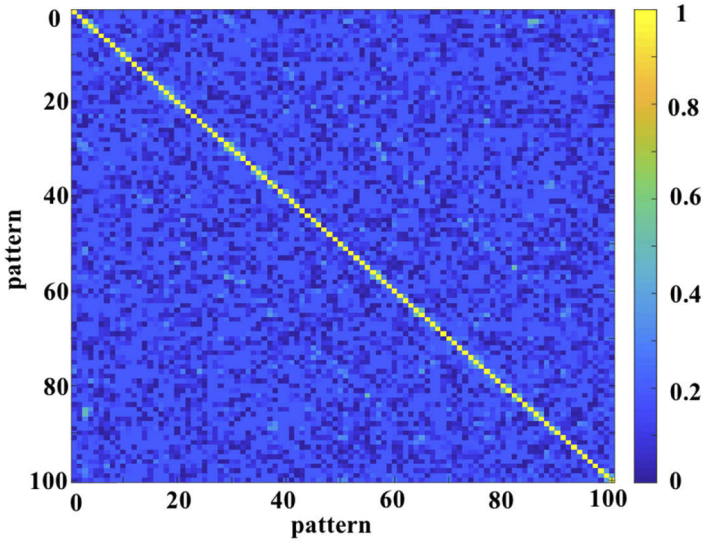


Fig. 3. Result of pattern correlation coefficient of continuous optical pulses that passed the cascaded MZIs.

from MLL is linked to the oscilloscope for synchronization. The time-stretched pulse with PRBS modulation goes through the optical circulator then emits into the open space via a collimator (Thorlabs, F240APC-1550). The optical pulses of the beam pass through a telescope set (two plano-convex lenses with focusing length of 50mm and 150mm, respectively), which is employed to expand to three times its beam size. The expanded and collimated beam scatters onto a diffraction grating (600 lines/mm), where the one-to-one mapping between wavelength and space is performed. Then the spectral encoded and random PRBS modulated pulses pass through the sample (1951 USAF resolution target), where the imaging and random patterns in spatial domain is mixed.

The optical pulses carrying the information of imaging and random patterns, and reflected by a silver-coated mirror, returned to the original collimator with same free-space optical way. The information-carried optical pulses in time-serial are detected by a single-pixel PD with a bandwidth of 2GHz via a circulator. An oscilloscope with a real-time sampling rating of 20GS/s and a bandwidth of 2GHz is employed to digitize the captured information followed by information processing in computer using Matlab programming. Note in this demonstration the data compressing of CS method is implemented in digital domain, that is to say, the pulse compression for every 20 ns is digitally-added in Matlab instead of using single-mode fiber (SMF) to compress the time-stretched optical pulse, which is limited by the existing devices. The setup of our optical imaging system can be easily improved by using matched length of SMF (around 20KM) to compensate the DCF and a low-cost 50MHz PD, thus the cost and data volume of system can be furtherly reduced.

To perform a fast CSI system, a fast galvo-scanner could be applied to change the height of time-stretched optical pulses that reach the sample or a mechanical scheme could be used to change the height of sample rapidly.

In our CS calculation, a 1D sample imaging $I_{M\times1}$ has a length of M points. And they are mixed with N random patterns that from the cascaded MZIs, N is the number of measurements (N < M). $I_{M\times1}$ can be expressed as

$$I_{M\times1} = \varphi_{M\times M} \times S_{M\times1} \tag{1}$$

Optics EXPRESS

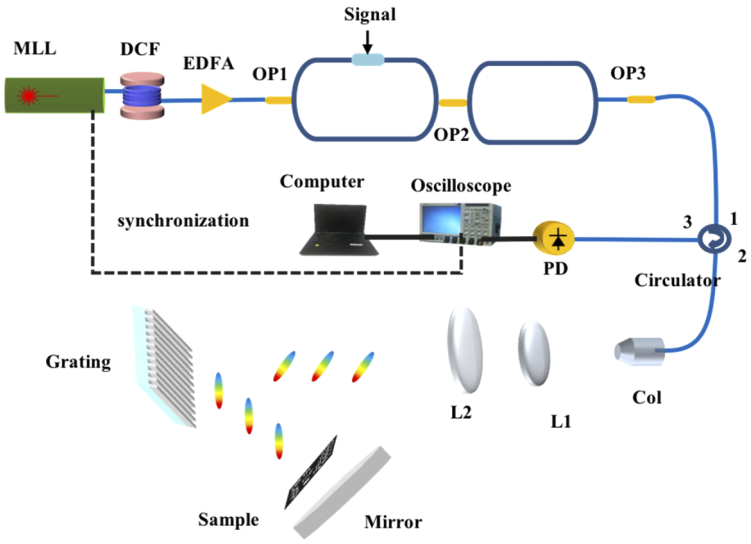


Fig. 4. Schematic of the proposed CSI system based on SETS structure. CSI: compressive sensing imaging; SETS: spectrum-encoded time-stretch; MLL: mode-locked laser; DCF: dispersive compensating fiber; EDFA: Erbium doped fiber amplifiers; OP: optical fiber coupler; L1 and L2: lens; PD: photodetector.

where $\varphi_{M\times M}$ is a M×M matrix stands for Fourier orthogonal basis, $S_{M\times 1}$ is a M×1 matrix stands for the spectrum of $I_{M\times 1}$ in transformation domain. Each pattern $R_{M\times 1}$ (also has a length of M points) on behalf of each measurement. The 1D sample imaging has to be sparse in discreet Fourier transformation (DFT) domain, N number of random patterns can be expressed as the M×N dimensional measurement matrix $R_{M\times N}$, and hence the measurement vector $y_{N\times 1}$ also known as dot product, is shown as

$$y_{N\times 1} = R_{N\times M} \times I_{M\times 1} = R_{N\times M} \times \varphi_{M\times M} \times S_{M\times 1} = \theta_{N\times M} \times S_{M\times 1} \tag{2}$$

where $\theta_{N\times M} = R_{N\times M} \times \varphi_{M\times M}$.

The imaging information recovery from $y_{N\times 1}$ to $I_{M\times 1}$ is a process of convex optimization. The measurement vector $y_{N\times 1}$, also known as the measurement results, and the random pattern matrix $R_{N\times M}$ (the random patterns that generated by the cascaded MZIs) are given as inputs from the proposed system. $\varphi_{M\times M}$ is a standard orthogonal basis, and the matrix product $\theta_{N\times M}$ is random, which has to meet the restricted isometry property [34]. As a result, an achievable and possible $S_{M\times 1}$ can be obtained when using total variation (TV) minimization algorithm based on minimum l_1 norm reconstruction [35,36],

$$s = \arg min(TV_1) \text{ subject to } \theta s = y \tag{3}$$

Based on the above analysis, the presentation of transformation domain s can be obtained. And the 1D imaging information can be reconstructed due to $I_{M\times 1} = \varphi_{M\times M} \times S_{M\times 1}$.

A simulation is performed based on the proposal. The imaging sample of 1951 USAF resolution target used in our proposed system to perform CSI is shown in Fig. 5(a). The imaging area is shown in the red line square with an area (field of view) of 0.6*2.2 mm and a dimension of 50 lines, 400 columns (M=400), which is group 2, number 2. Figure 5(b) and (c) illustrated the results of reconstructed 2D image (based on minimum l_1 norm reconstruction) areas using different numbers of random patterns or times of measurement, which are 100 and 50 (N=100, 50), and the data compression ratio are 25% and 12.5%, respectively. Figure 5(d) and (e) are the

Optics EXPRESS

reconstructed lines (red color) and original lines (blue color) of line 10 and line 26, respectively in image (b), which show in good consistency. From Fig. 5(b) and (c), when 100 or 50 (N=100, 50) times of measurement/random patterns are employed in our proposed CSI system, the target data stream with recovered a set of 400 (M=400) data matched the original imaging line, which confirms our proposal for CSI approach is applicable.

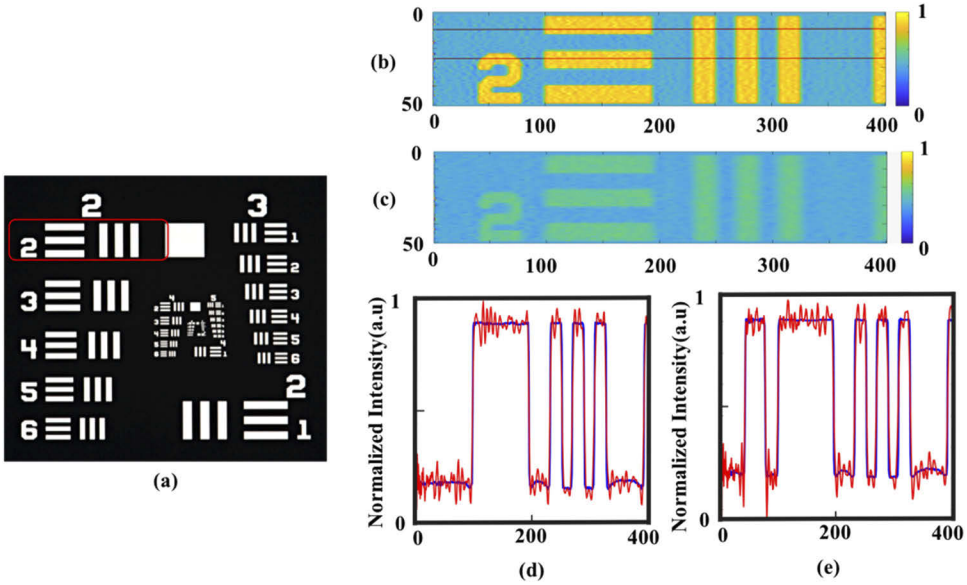


Fig. 5. The simulation result for CSI system. (a) The imaging sample of 1951 USAF resolution target, red square is the imaging area. Based on minimum l_1 norm reconstruction, the simulation results of reconstructed images with (b)100 and (c) 50 times of measurements have data compression ratio of 25% and 12.5%, respectively. (d) and (e) are the simulation results of reconstructed lines (red color) and original lines (blue color) of line 10 and line 26, respectively in image (b).

A proof-of-principle experiment is performed to confirm our proposal. Based on the imaging system in Fig. 4, the imaging results with same imaging area in Fig. 5(a) are shown in Fig. 6. Figure 6(a) and (b) show the experimental results of reconstructed images with 100 and 50 times of measurements, which have data compression ratio of 25% and 12.5%, respectively. Figure 6(c) and (d) are the experimental results of reconstructed line 10 and line 26, respectively in image Fig. 6(a). The results of Fig. 6(a) and (b) show when using 100 or 50 (N=100, 50) times of measurement/random patterns, an imaging set of 400 (M=400) data can be recovered in our proposed CSI system. Simulation and experiment of our proposed CSI system with data compression ratio of 10% and 6% are shown in Fig. 7. The Fig. 7(a) and 7(b) show the reconstructed image (with pixel size of 50*400) in simulation and experiment with 40 times of measurements (data compression ratio of 10%). The Fig. 7(c) and 7(d) show the reconstructed image (with pixel size of 50*400) in simulation and experiment with 24 times of measurements (data compression ratio of 6%). In our situation, the image can reconstructed with good performance of 10%. And with 6% of data compression ratio, the image can still get reconstructed.

Optics EXPRESS

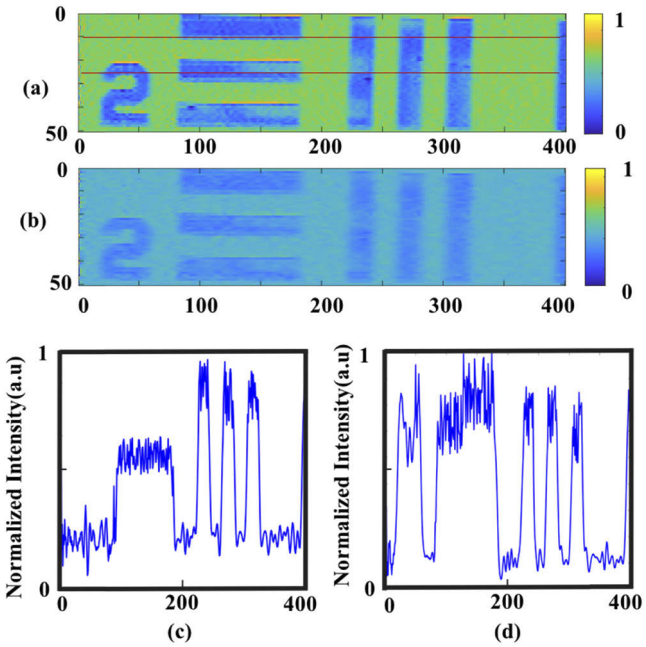


Fig. 6. The experimental result for CSI system. The experimental results of reconstructed images with (a)100 and (b) 50 times of measurements have data compression ratio of 25% and 12.5%, respectively. (c) and (d) are the experimental results of reconstructed line 10 and line 26, respectively in image (a).

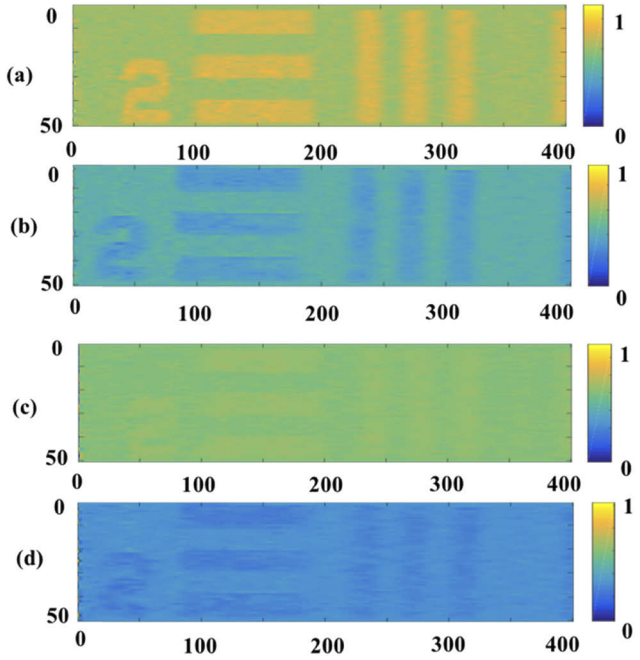


Fig. 7. (a) simulation and (b) experimental results of CSI system with data compression ratio of 10% ; (c) simulation and (d) experimental results of CSI system with data compression ratio of 6%.

Optics EXPRESS

3. Conclusion

In summary, we proposed and experimentally demonstrated a low-cost and easy-access optical CSI system using SETS structure with potential dynamic phenomena detection. The cascaded MZIs based optical random pattern generator is applied for low-cost optical mixing, and no expensive electro-optical modulator is involved. The experimental result of CSI system shows a data compression ratio from 6% to 25% is performed using a computational low-speed data acquisition at 50MS/s in Matlab. The proposed system could solve the big data issue in the traditional data acquisition procession, and reduce the cost of system using low-bandwidth PD and oscilloscope. Our proposal provide a data efficient, cost-efficient and accessible approach makes dynamic phenomena detection and measurement possible.

Funding. Engineering and Physical Sciences Research Council (EP/T51732X/1); National Natural Science Foundation of China (61975248, LZC0019, LZC0020, Y01236128).

Disclosures. The authors declare that there are no conflicts of interest related to this article.

References

1. K. Goda, K. K. Tsia, and B. Jalal, "Serial Time-Encoded Amplified Imaging for Real-Time Observation of Fast Dynamic Phenomena," Nature **458**(7242), 1145–1149 (2009).
2. K. Goda, A. Mahjoubfar, C. Wang, A. Fard, J. Adam, D. R. Gossett, A. Ayazi, E. Sollier, O. Malik, E. Chen, Y. Liu, R. Brown, N. Sarkhosh, D. Di Carlo, and B. Jalali, "Hybrid Dispersion Laser Scanner," Sci. Rep. **2**(1), 445 (2012).
3. K. Goda, A. Ayazi, D. R. Gossett, J. Sadasivam, C. K. Lonappan, E. Sollier, A. M. Fard, S. C. Hur, J. Adam, C. Murray, C. Wang, N. Brackbill, D. Di Carlo, and B. Jalali, "High-throughput single-microparticle imaging flow analyzer," Proc. Natl. Acad. Sci. U. S. A. **109**(29), 11630–11635 (2012).
4. G. Wang, C. Wang, Z. Yan, and L. Zhang, "Highly efficient spectrally encoded imaging using a 45° tilted fiber grating," Opt. Lett. **41**(11), 2398–2401 (2016).
5. G. Wang, Z. Yan, L. Yang, L. Zhang, and C. Wang, "Improved Resolution Optical Time Stretch Imaging Based on High Efficiency In-Fiber Diffraction," Sci. Rep. **8**(1), 600 (2018).
6. M. P. Edgar, G. M. Gibson, and M. J. Padgett, "Principles and prospects for single-pixel imaging," Nat. Photonics **13**(1), 13–20 (2019).
7. G. Wang and C. Wang, "Diffraction Limited Optical Time-Stretch Microscopy Using an In-Fibre Diffraction Grating," in *Frontiers in Optics/Laser Science 2016* (Optical Society of America, 2016), Rochester, United States, 2016.
8. G. Pu, L. Yi, L. Zhang, C. Luo, Z. Li, and W. Hu, "Intelligent control of mode-locked femtosecond pulses by time-stretch-assisted real-time spectral analysis," Light: Sci. Appl. **9**(1), 13 (2020).
9. C. Lei, B. Guo, Z. Cheng, and K. Goda, "Optical time-stretch imaging: Principles and applications," Appl. Phys. Rev. **3**(1), 011102 (2016).
10. C. Lei, H. Kobayashi, Y. Wu, M. Li, A. Isozaki, A. Yasumoto, H. Mikami, T. Ito, N. Nitta, T. Sugimura, M. Yamada, Y. Yatomi, D. Carlo, Y. Ozeki, and K. Goda, "High-throughput imaging flow cytometry by optofluidic time-stretch microscopy," Nat. Protoc. **13**(7), 1603–1631 (2018).
11. J. Wu, Y. Xu, J. Xu, X. Wei, A. C. S. Chan, A. H. L. Tang, A. K. S. Lau, B. M. F. Chung, H. Shum, E. Y. Lam, K. K. Y. Wong, and K. K. Tsia, "Ultrafast laser-scanning time-stretch imaging at visible wavelengths," Light: Sci. Appl. **6**(1), e16196 (2017).
12. F. Xing, H. Chen, C. Lei, Z. Weng, M. Chen, S. Yang, and S. Xie, "Serial wavelength division 1 GHz line-scan microscopic imaging "," Photonics Res. **2**(4), B31–B34 (2014).
13. A. K. S. Lau, T. T. W. Wong, K. K. Y. Ho, M. T. H. Tang, A. C. S. Chan, X. Wei, E. Y. Lam, H. C. Shum, K. K. Y. Wong, and K. K. Tsia, "Interferometric time-stretch microscopy for ultrafast quantitative cellular and tissue imaging at 1 μm "," J. Biomed. Opt. **19**(7), 076001 (2014).
14. L. Y. Shao, S. Q. Liu, S. Bandyopadhyay, F. H. Yu, W. J. Xu, C. Wang, H. C. Li, M. I. Vai, L. L. Du and J, and S. Zhang, "Data-driven Distributed Optical Vibration Sensors: A Review," IEEE Sens. J. **20**(12), 6224–6239 (2020).
15. H. He, L.-Y. Shao, H. Li, W. Pan, B. Luo, X. Zou, and L. Yan, "SNR enhancement in phase-sensitive OTDR with adaptive 2D bilateral filtering algorithm," IEEE Photonics J. **9**(3), 1–10 (2017).
16. Y. Jiang, S. Karpf, and B. Jalali, "Time-stretch LiDAR as a spectrally scanned time-of-flight ranging camera," Nat. Photonics **14**(1), 14–18 (2020).
17. C. K. Mididoddi, F. Bai, G. Wang, C. Liu, S. Gibson, and C. Wang, "High-Throughput Photonic Time-Stretch Optical Coherence Tomography with Data Compression," IEEE Photonics J. **9**(4), 1–15 (2017).
18. C. K. Mididoddi, G. Wang, and C. Wang, "Data compressed photonic time-stretch optical coherence tomography," in *Proc. IEEE Photon. Conf., 2016*, Waikoloa, HI, USA, 2016
19. B. T. Bosworth, J. R. Stroud, D. N. Tran, T. D. Tran, S. Chin, and M. A. Foster, "High-speed flow microscopy using compressed sensing with ultrafast laser pulses," Opt. Express **23**(8), 10521–10532 (2015).
20. G. J. Tearney, M. Shishkov, and B. E. Bouma, "Spectrally Encoded Miniature Endoscopy," Opt. Lett. **27**(6), 412–414 (2002).

Optics EXPRESS

21. G. Wang, U. Habib, Z. Yan, N. J. Gomes, Q. Sui, J. Wang, L. Zhang, and C. Wang, "Highly efficient optical beam steering using an in-fiber diffraction grating for full duplex indoor optical wireless communication," J. Lightwave Technol. **36**(19), 4618–4625 (2018).
22. G. Wang, U. Habib, C. Wang, N. J. Gomes, Z. Yan, and L. Zhang, "Wavelength-controlled beam steering for optical wireless transmission using an in-fiber diffraction grating," in *Conference on Lasers and Electro-Optics*, San Jose, California, USA, 2017, p. SF1L.5.
23. S. Bandyopadhyay, L. Shao, W. Chao, Z. Yan, F. Hong, G. Wang, J. Jiang, P. Shum, X. Hong, and W. Wang, "Highly efficient free-space fiber coupler with 45 tilted fiber grating to access remotely placed optical fiber sensors," Opt. Express **28**(11), 16569–16578 (2020).
24. G. Wang, L. Shao, D. Xiao, S. Bandyopadhyay, J. Jiang, S. Liu, W. Li, C. Wang, and Z. Yan, "Stable and Highly Efficient Free-Space Optical Wireless Communication System Based on Polarization Modulation and In-Fiber Diffraction," J. Lightwave Technol. **39**(1), 83–90 (2021).
25. A. Mahjoubfar, C. L. Chen, and B. Jalali, "Design of Warped Stretch Transform," Sci. Rep. **5**(1), 17148 (2015).
26. B. Jalali and M. H. Asghari, "The Anamorphic Stretch Transform: Putting the Squeeze on "Big Data"," Opt. Photonics News **25**(2), 24–31 (2014).
27. Q. Guo, H. Chen, Z. Weng, M. Chen, S. Yang, and S. Xie, "Compressive sensing based high-speed time-stretch optical microscopy for two-dimensional image acquisition," Opt. Express **23**(23), 29639–29646 (2015).
28. C. Lei, Y. Wu, A. Sankaranarayanan, S. Chang, B. Guo, N. Sasaki, H. Kobayashi, C. Sun, Y. Ozeki, and K. Goda, "GHz optical time-stretch microscopy by compressive sensing," IEEE Photonics J. **9**(2), 1–8 (2017).
29. J. Shin, B. T. Bosworth, and M. A. Foster, "Single-pixel imaging using compressed sensing and wavelength-dependent scattering," Opt. Lett. **41**(5), 886–889 (2016).
30. C. K. Mididoddi, E. J. Ahmad, and C. Wang, "All-Optical Random Sequence Generation For Compressive Sensing Detection of RF Signals," in *2017 International Topical Meeting on Microwave Photonics (MWP)*, Beijing, China, 2017.
31. N. Jing, C. K. Mididoddi, and C. Wang, "Compressive Sensing Detection of RF Signals by All-Optically Generated Binary Random Patterns," in *2019 IEEE 2nd British and Irish Conference on Optics and Photonics (BICOP)*, London, UK, 2019.
32. H. He, L. Y. Shao, B. Luo, Z. Li, X. Zou, Z. Zhang, W. Pan, and L. Yan, "Multiple vibrations measurement using phase-sensitive OTDR merged with Mach-Zehnder interferometer based on frequency division multiplexing," Opt. Express **24**(5), 4842–4855 (2016).
33. G. Wang, T. Xu, and F. Li, "PGC Demodulation Technique With High Stability and Low Harmonic Distortion," IEEE Photonics Technol. Lett. **24**(23), 2093–2096 (2012).
34. E. J. Candes and T. Tao, "Decoding by linear programming," IEEE Trans. Inf. Theory **51**(12), 4203–4215 (2005).
35. J. A. Tropp, J. N. Laska, M. F. Duarte, J. K. Romberg, and R. G. Baraniuk, "Beyond Nyquist: Efficient sampling of bandlimited signals," IEEE Trans. Inf. Theory **56**(1), 520–544 (2010).
36. D. Rontani, D. Choi, C. Y. Chang, A. Locquet, and D. S. Citrin, "Compressive Sensing with Optical Chaos," Sci. Rep. **6**(1), 35206 (2016).